In Vivo Use of a Radioiodinated Somatostatin Analogue: Dynamics, Metabolism, and Binding to Somatostatin Receptor-Positive Tumors in Man

Willem H. Bakker, Eric P. Krenning, Wout A. Breeman, Peter P. M. Kooij, Jean-Claude Reubi, Jan W. Koper, Marion de Jong, Johannes S. Laméris, Theo J. Visser, and Steven W. Lamberts

Departments of Nuclear Medicine, Internal Medicine III, and Radiology, University Hospital Dijkzigt and Erasmus University Medical School, Rotterdam, The Netherlands; and Sandoz Research Institute, Berne, Switzerland

Somatostatin analogues, labeled with gamma-emitting radionuclides, are of potential value in the localization of somatostatin receptor-positive tumors with gamma camera imaging. We investigated the application in man of a radioiodinated analogue of somatostatin, ^{123}I-Tyr-3-octreotide, which has similar biologic characteristics as the native peptide. The radiopharmaceutical is cleared rapidly from the circulation (up to 85% of the dose after 10 min) mainly by the liver. Liver radioactivity is rapidly excreted into the biliary system. Until 3 hr after injection, radioactivity in the circulation is mainly in the form of ^{123}I-Tyr-3-octreotide. Thereafter, plasma samples contain increasing proportions of free iodide. Similarly, during the first hours after injection, radioactivity in the urine exists mainly in the form of the unchanged peptide. Thereafter, a progressive increase in radioiodide excretion is observed, indicating degradation of the radiopharmaceutical in vivo. Fecal excretion of radioactivity amounts to only a few percent of the dose. The calculated median effective dose equivalent is comparable with values for applications of other ^{123}I-radiopharmaceuticals (0.019 mSv/MBq).

J Nucl Med 1991; 32:1184–1189

Somatostatin is a peptide hormone that exerts a wide variety of actions throughout the body. It plays an inhibitory role in the normal regulation of several organ systems, including the central nervous system, the hypothalamus, the pituitary gland, the gastrointestinal tract, and the endocrine and exocrine pancreas (*1,2*). Large numbers of binding sites with a high affinity for somatostatin have been detected with in vitro techniques in many tumors arising from these organ systems; these include pituitary tumors (*3*), brain tumors such as meningiomas and low-grade astrocytomas (*4,5*), and hormone-producing tumors in the gastrointestinal tract including the pancreas (*6,7*).

Received Jun. 27, 1990; revision accepted Nov. 19, 1990.

For reprints contact: Willem H. Bakker, University Hospital Dijkzigt, Department of Nuclear Medicine, Dr Molewaterplein 40, 3015 GD Rotterdam, The Netherlands.

It has previously been shown in animal studies that it is possible to detect somatostatin receptors in vivo after administration of ^{123}I-Tyr-3-octreotide to somatostatin receptor-positive tumor-bearing rats (*8*).

It has also been shown in a preliminary study that the in vivo application of the same radiopharmaceutical in man results in scintigraphic imaging of somatostatin receptor-positive tumors (*9*). In this study, we present data on the metabolism of intravenously administered ^{123}I-Tyr-3-octreotide in man and estimates of the radiation dose. Also, scintigraphy is shown of a patient with two different somatostatin receptor-positive tumors.

MATERIALS AND METHODS

Radiopharmaceuticals

Radioiodination of Tyr-3-octreotide was performed with the chloramine-T method as described previously (*8*). Specific activities ranged from 18.5 to 37 MBq/μg (0.5–1 mCi/μg) of ^{123}I-Tyr-3-octreotide. Images were obtained after intravenous injection of 370–555 MBq (10–15 mCi; 15–25 μg) ^{123}I-labeled somatostatin analogue. To prevent accumulation of radioiodine in the thyroid, patients were given daily 3 × 50 mg potassium iodide and 4 × 250 mg potassium perchlorate for 3 days, starting 1 day before injection of ^{123}I-Tyr-3-octreotide.

Imaging

Planar and SPECT images were obtained with a large field of view gamma camera (Counterbalance 3700 and ROTA-II, Siemens) equipped with a 190-keV parallel-hole collimator. The analyzer was set to 159 keV with a 20% window. Data were stored in a dedicated computer (Gamma-11, Nuclear Diagnostics, Hägersten, Sweden). During the first 30 min of the study, computer images (matrix 64 × 64) were acquired in 40 intervals of 3 sec each and 28 intervals of 1 min each. Analogue images were made at regular intervals during the first 30 min. Anterior and posterior whole-body scintigraphy were performed 30 min after injection. Images (both analogue and digital, matrix 128 × 128) also were obtained at approximately 4 and 24 hr after injection. In a few cases, scintigraphy also was performed after 2 and 48 hr. SPECT was always performed for localization of primary tumors in the head/neck region as well as in cases of overprojection of the tumor with normal tissue (e.g., liver and kidneys). SPECT reconstruction images were made at 60 angles for 360°. Acquisi-

tion time per angle was always 30 sec. The original data were prefiltered with a Wiener filter. The filtered data were reconstructed with a Ramp filter. The reconstruction program (SPETS version 6.01) was obtained from Nuclear Diagnostics.

Measurements of Radioactivity in Blood, Urine, and Feces

The radioactivity in blood, urine, and feces was measured with a LKB-1282-Compugamma system or a GeLi-detector equipped with a multichannel analyzer (Series 40, Canberra). Blood samples were collected directly before injection and after 2, 5, 10, 20, 40, 60, 90 min and 2, 3, 5, 8 and 20 hr. Urine was collected in 5-hr intervals until 50 hr after injection. If feasible feces were not collected until 48 hr after injection.

The chemical status of the radionuclide in blood and urine was analyzed as function of time by using the SEP-PAK C18, HPLC and gel filtration techniques described previously (*8*). The nature of peptide-bound radioactivity in blood and urine was tested by investigation of specific binding to human meningioma membranes as described previously (*4*).

Patients

Kinetic studies with ^{123}I-Tyr-3-octreotide by means of gamma camera scintigraphy were performed in 13 patients with several types of tumors, including endocrine pancreatic tumors, metastatic carcinoids, and meningiomas. Additionally, plasma, urine, and feces samples were obtained from seven, eight, and seven patients, respectively.

Dosimetry

For the estimation of the radiation dose the MIRDOSE version 2 program (*10*) and ICRP publication 53 (*11*) were used. The dose estimates were calculated on the basis of the following. The uptakes in the most important source organs, the gallbladder, the liver, and the total body, were determined as a function of time. Radioactivity in the liver and the gallbladder was calculated using the geometric mean of anterior and posterior counts. Patient overall thickness, for attenuation correction, was determined from a lateral view and was assumed to be constant over the abdomen. An anatomic liver phantom contained in a water bath was used to calculate the effects of the object geometry (*12*). The water thickness was varied from 15 to 20 cm, a typical patient range.

Calibrated amounts of radioactivity were placed in the liver phantom and in a standard bottle. The standard bottle was placed on top of the collimator and counts were determined from one view. From calculated counts in the liver phantom and measured counts in the standard bottle, a geometry factor was determined as a function of the water thickness. Because of the observed small variations in the geometry factor, as a function of water thickness, a constant was used to calculate the absolute uptake of the radionuclide in the liver (*13*). The gallbladder was regarded to have the same geometry as the standard bottle. A geometry factor for the intestines could not be determined but was taken to be the same as for the liver. In order to quantitate the percentage uptake in the various organs, a standard bottle containing an aliquot of the injected dose was measured just before each patient study. Background correction for the liver was performed on the basis of an area just outside the liver region. Background correction for the gallbladder was performed on the basis of a region within the liver next to the gallbladder.

For dosimetry, the biologic half-life of the liver activity was calculated by analysis of the computer images 4 and 24 hr after injection. The biologic half-life in the gallbladder could not be measured, but was estimated to be 2.5 hr based upon experimental circumstances and the literature (*11*). No predominant accumulation of radioactivity was seen in organs other than liver and gallbladder during patient studies. Other organs therefore were disregarded as source organs except that the uptake of radioactivity in the total body was assumed to be 100% minus the uptake in the liver, gallbladder, and collected urine together. Since urine data were not available for all patients, it was assumed for dose calculations that the activity in the urine for these patients was equal to the mean activity in the urine for the eight patients with correct urine collection. Furthermore, dosimetry calculations were performed on an individual basis.

RESULTS

In seven consecutive patients injected with ^{123}I-Tyr-3-octreotide, the average plasma radioactivity decreased rapidly after injection. Assuming a plasma volume of 3 liters, the radioactivity in the circulation was calculated to decrease within 10 min to less than 15% (s.d. 5%) of the dose. In two patients, the chemical status of the radionuclide in the plasma was investigated as a function of time. During the first hours, plasma radioactivity was mostly peptide-bound. After 3 hr, the peptide-bound fraction of total radioiodide was still about 70%. In Figure 1, the time course of total and peptide-bound radioactivity is presented during the first 5 hr after injection of ^{123}I-Tyr-3-octreotide.

The urinary excretion of radioactivity in eight patients was measured by collecting samples at 5-hr intervals. Figure 1 (inset) shows that about 45% of the administered

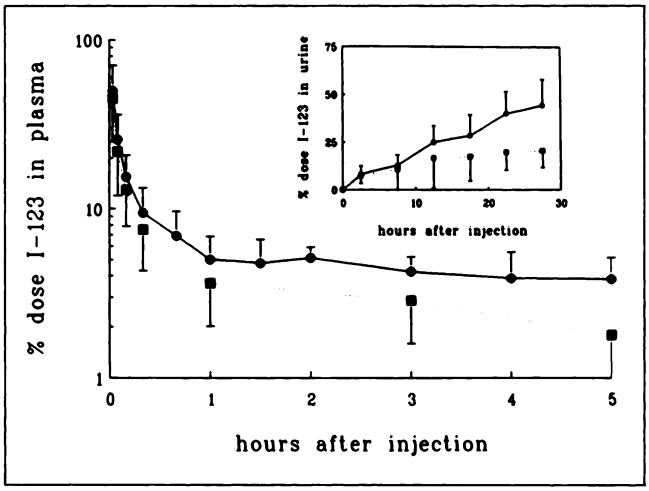

FIGURE 1. Total plasma radioactivity (●) after administration of ^{123}I-Tyr-3-octreotide in seven patients. Peptide-bound (■) radioactivity was calculated on the basis of data from two patients. Data are expressed as percentage (mean ± s.d.) of the dose. (Inset) Cumulative total ^{123}I-excretion (●) in the urine after intravenous injection of ^{123}I-Tyr-3-octreotide in eight patients. Cumulative peptide-bound radioactivity (■) was calculated on the basis of data obtained from four patients. Data are expressed as percentage (mean ± s.d.) of the dose.

dose was excreted in the urine within 30 hr after injection. The chemical status of the radionuclide in the urine was investigated as a function of time. Figure 1 (inset) also shows that in four of the patients mainly peptide-bound activity was excreted during the first 10 hr after injection. Thereafter, a progressive increase in radioiodide excretion was observed.

In four patients with a normal intestinal function, feces were not collected until 48 hr after injection of ^{123}I-Tyr-3-octreotide contained less than 2% of the administered radioactivity. However, in another three patients with abnormal intestinal function (e.g., due to previous intestinal surgery), 20%–45% of the administered radioactivity was excreted in the feces within 48 hr after injection. This difference in fecal excretion was in accordance with scintigraphy, showing more radioactivity in the colon of the patients with abnormal intestinal function compared with patients with normal intestinal function. Figure 2A is an example of a patient with a disturbed intestinal function (after total gastrectomy and partial removal of the duodenum), which clearly shows the presence of radioactivity in the colon.

The SEP-PAK C18 and HPLC-purified radiolabeled-peptide component in plasma and urine showed the same biologic activity as the radiopharmaceutical itself as indicated by its specific binding to human meningioma membranes (data not shown).

After the intravenous administration of ^{123}I-Tyr-3-octreotide scintigraphy demonstrated that radioactivity was rapidly cleared from the circulation, as measured by a decreasing blood-pool activity over the cardiac region. Gamma camera images showed that at the same time the radiopharmaceutical accumulates rapidly in the liver, immediately followed by appearance in the biliary system and eventually in the small intestines, confirming the data of our animal experiments (*8*).

The calculated uptakes in liver and gallbladder, which varied strongly between patients, reached their highest values between 0.5 and 1.5 hr after injection of ^{123}I-Tyr-3-octreotide. After an initial rapid passage through the liver, the median radioactivity in the liver decreased to 28% of the dose (range 13%–41%) 4 hr after injection, and 6% of the dose (range 2%–17%) after 24 hr. Radioactivity in the gallbladder could already be observed after 5 min. After 4 hr, the accumulation in the gallbladder was 18% of the dose (range 3%–35%). Radioactivity in the gallbladder had disappeared after 24 hr. After 4 hr, less than 2% of the dose was measured in the intestines. In patients without tumors in the intestinal region and in patients who did not undergo intestinal surgery, some activity was measured in this area (median 6%, range 2%–9%) after 24 hr. Because of the short physical half-life of the ^{123}I and the low intestinal residence time, the intestines were disregarded as source organ in dosimetry. The calculated uptake in the total body in individual patients did not show a significant decrease from 4 to 24 hr after injection. For this reason, in the dose calculations the effective half-life for the total body was the same as the physical half-life of ^{123}I. Patients were investigated under maximum thyroid-blocking conditions to prevent accumulation of the radionuclide in the thyroid. Therefore, the circulating free radioiodide, released from the radiolabeled analogue, was largely cleared by the kidneys. Indeed, only very low thyroidal accumulation was seen. Consequently, the radiation dose to the thyroid was negligible and was not considered in the calculations. The kidneys, the intestines, and the bladder were sometimes seen on the gamma camera images but treated as negligible source organs because of the short residence time of the radionuclide in these organs. The results of the dosimetry are shown in Table 1.

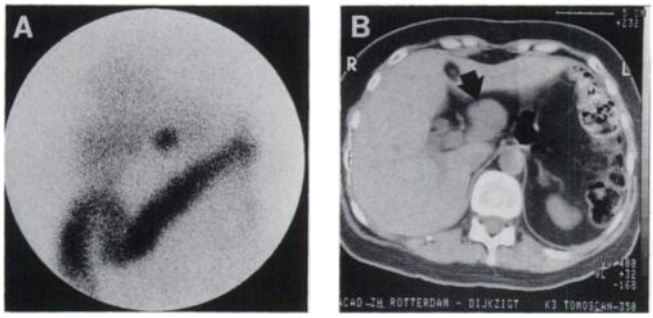

FIGURE 2. (A) Anterior abdominal image of somatostatin receptor-positive gastrinoma, taken 28 hr after injection of ^{123}I-Tyr-3-octreotide in a patient after gastrectomy and intestinal surgery. (B) CT scan of the abdomen with a slice at the level of the hot spot in Figure 2A showing an enlarged lymph node containing a gastrinoma metastasis (see arrow).

Case History

As an example, the detection of two different somatostatin receptor-positive tumors in one patient is presented. The patient, a 40-yr-old woman, underwent a total gastrectomy, subtotal pancreatectomy, and partial removal of the duodenum because of a large gastrin-secreting tumor in the cauda and corpus of the pancreas as well as in the wall of the duodenum at age 34. In the last 4 yr, serum gastrin levels increased steadily to levels 20 times above the upper limit of normal. This suggested the recurrence of gastrin-secreting tumor tissue, but its location could not be established immediately. In addition, this patient had a meningioma located parasellarly on the right side, which was removed at age 36. This tumor recurred, causing loss of vision of the right eye.

The presence of a somatostatin receptor-positive tumor (diameter 5 cm), which was subsequently shown to be a single gastrinoma-containing lymph node, was seen 3 min after injection of ^{123}I-Tyr-3-octreotide (not shown here) and was still clearly visible after 28 hr. Figure 2A shows the gastrinoma together with colon radioactivity and decreased liver activity on an anterior abdominal image 28 hr after injection of ^{123}I-Tyr-3-octreotide. Figure 2B shows this gastrinoma on the CT scan. At abdominal surgery, no

TABLE 1
Dose Estimates After Intravenous Administration of ^{123}I-Tyr-3-octreotide in Man on the Basis of Gamma Camera Measurements (n = 13) and Measurements of Urinary Excretion (n = 8)

Target organ	median absorbed dose (mGy/MBq)	range (mGy/MBq)
Gallbladder wall	0.119	0.043 - 0.222
Liver	0.048	0.024 - 0.081

Median effective dose equivalent (mSv/MBq)	range (mSv/MBq)
0.019	0.015 - 0.028

other gastrinoma metastases were found in the abdomen or in the liver.

Figures 3A-B (24 hr after administration of ^{123}I-Tyr-3-octreotide) indicate the existence of another lymph node metastasis of the gastrinoma on the left side of the mediastinum, while the somatostatin receptor-positive meningioma is also clearly visualized. Figures 3C-D present CT images of the lymph node metastasis and the meningioma, respectively.

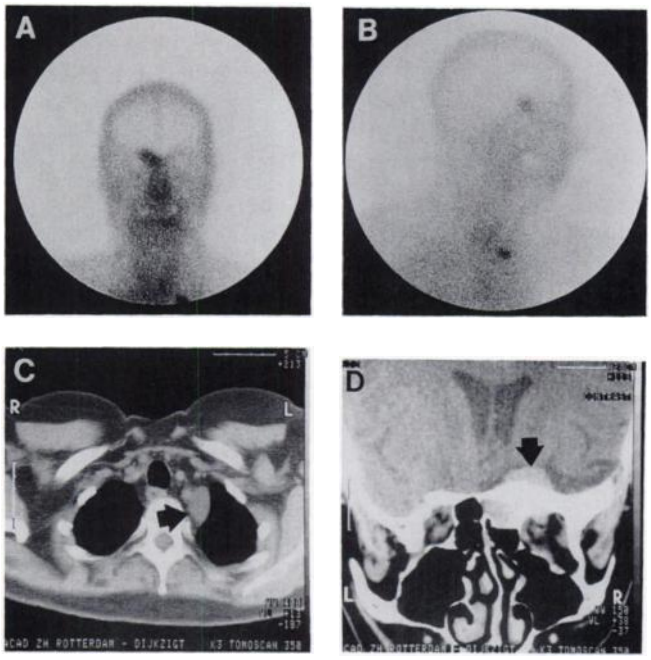

FIGURE 3. (A) Anterior scintigraphy of a lymph node metastasis of the gastrinoma (on the left side of the mediastinum) and a meningioma 24 hr after injection of ^{123}I-Tyr-3-octreotide. (B) Right lateral scintigraphy of the lymph node metastasis and the meningioma. (C) CT scan of a lymph node metastasis of the gastrinoma in the mediastinum (see arrow). (D) CT scan of the somatostatin receptor-positive meningioma (see arrow).

DISCUSSION

Tyr-3-octreotide, labeled with ^{125}I, which is successfully applied to in vitro somatostatin receptor studies, is not suitable for in vivo imaging because of the low-energy gamma emissions of ^{125}I. Although the radiation emitted by ^{131}I is more favorable for scintigraphy, the disadvantage that this isotope shares with ^{125}I is its low specific activity (*14*), which necessitates purification of the radioiodination products by HPLC and lowers the yield of monoiodinated Tyr-3-octreotide especially when the usual, low amounts of peptide are labeled. However, with the availability of cyclotron-produced ^{123}I (half-life 13.2 hr, gamma energy 159 keV), efficient radiolabeling of Tyr-3-octreotide is possible (*8*), enabling excellent imaging including SPECT. Because of its short half-life it is possible to administer high doses (maximal 555 MBq ^{123}I was used), while the dose equivalent to the patient can be kept within regular limits of common nuclear medicine studies.

The metabolism of intravenously administered radioiodinated Tyr-3-octreotide in man is primarily characterized by a rapid clearance by the liver, immediately followed by biliary excretion into the small intestine. On the basis of preliminary rat liver perfusion experiments (Bakker WH et al, unpublished data), it is presumed that ^{123}I-Tyr-3-octreotide is excreted intact through the bile in man. The degradation of ^{123}I-Tyr-3-octreotide in the intestines is uncertain, but presumably the compound is hydrolyzed and its degradation products are enterally absorbed like those of octreotide (*15*). Thereafter, deiodination happens in tissues after which free radioiodide is ultimately cleared via the kidneys. This is supported by the observations in our patients that nearly all excreted radioactivity is present

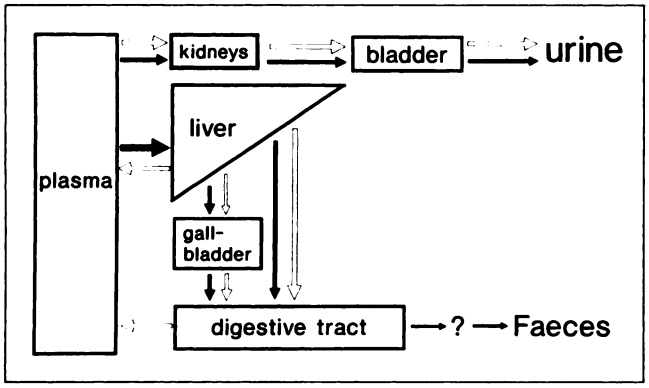

FIGURE 4. Hypothetical model of the metabolism of ^{123}I-Tyr-3-octreotide (closed arrows), ^{123}I-Tyr-3-octreotide, and (open arrows) degradation products of ^{123}I-Tyr-3-octreotide including free iodide.

in the urine and normally only a very small amount is found in the feces, despite considerable biliary excretion. Exceptions are patients with previous intestinal operations leading to a short bowel syndrome as in the case presented in Figure 2A.

Analysis of the chemical status of plasma radioactivity in the samples of the first 3 hr after injection mainly shows peptide-bound radioiodine in the form of the original ^{123}I-Tyr-3-octreotide. Analysis of radioactivity in the urine as a function of time predominantly shows intact ^{123}I-Tyr-3-octreotide during the first 10 hr after injection. In the subsequent samples, more and more free radioiodide is found. This free iodide is excreted over a long time course. These observations clearly indicate an effective deiodination of the injected compound and/or its degradation products in vivo. On the basis of these data a metabolic model is presented in Figure 4.

In order to visualize a tumor by receptor binding of ^{123}I-Tyr-3-octreotide, the specific activity expressed in counts per unit of area must exceed the local background radiation. For instance, in the hepatic region tumor receptor accumulation is more difficult to visualize during the period of normal hepatic uptake of the radioligand. The rapidly decreasing background activity (also in the liver area due to biliary excretion) facilitates the detection and localization of somatostatin receptor-positive tumors, which is further improved by the use of SPECT.

We previously reported successful imaging with this procedure of various somatostatin receptor-positive tumors, including endocrine pancreatic tumors, carcinoids, meningiomas, small-cell cancers of the lung, neuroblastomas, paragangliomas, pheochromocytomas, astrocytomas, and some hormone-producing pituitary tumors (*9,16–19*).

The advantage of this technique compared with currently available diagnostic radiologic procedures is evident. ^{123}I-Tyr-3-octreotide scintigraphy is a convenient, painless, and harmless technique without side effects and with an acceptable effective dose equivalent, comparable with values for other ^{123}I-labeled radiopharmaceuticals (*11*). Apart from the detection of previously often unknown metastases or multiple-tumor localizations with whole-body scintigraphy, the visualization of somatostatin receptor-positive tumors may predict the possible success of octreotide radiotherapy. Although ^{131}I is an attractive radionuclide for this purpose, its low specific activity would necessitate the administration of very high amounts (milligrams) of Tyr-3-octreotide required for binding of therapeutic amounts of ^{131}I. However, somatostatin analogues radiolabeled with an ultra pure short-lived alpha or beta emitter are potential, new therapeutic radiopharmaceuticals in the treatment of somatostatin receptor-positive cancer.

ACKNOWLEDGMENTS

The authors thank Ina Loeve, Marcel van der Pluijm, Yolanda de Graaf, and René Rijsdijk for expert technical assistance.

REFERENCES

1. Reichlin S. Somatostatin. *N Engl J Med* 1983;309:1495–1501, 1556–1563.
2. Lamberts SWJ. Therapeutic effects of somatostatin analogs. *ISI Atlas of Science: Pharmacology* 1988:179–184.
3. Reubi JC, Landolt AM. High density of somatostatin receptors in pituitary tumors from acromegalic patients. *J Clin Endocrinol Metab* 1984;59:1148–1151.
4. Reubi JC, Maurer R, Klijn JGM, Stefanko SZ, Foekens JA, Blaauw G, et al. High incidence of somatostatin receptors in human meningiomas: biochemical characterization. *J Clin Endocrinol Metab* 1986;63:433–438.
5. Reubi JC, Horisberger U, Lang W, et al. Coincidence of EGF receptors and somatostatin receptors in meningiomas but inverse, differentiation-dependent relationship in glial tumors. *Am J Pathol* 1989;134:337–344.
6. Reubi JC, Häcki WH, Lamberts SWJ. Hormone-producing gastrointestinal tumors contain a high density of somatostatin receptors. *J Clin Endocrinol Metab* 1987;65:1127–1134.
7. Reubi JC, Kvols L, Charboneau W, Reading C, Moertel C. Carcinoid tumors have a high density of somatostatin receptors that may be assessed by percutaneous needle biopsy. *Proc Am An Cancer Res* 1989;30:308.
8. Bakker WH, Krenning EP, Breeman WA, et al. Receptor scintigraphy with a radioiodinated somatostatin analogue: radiolabeling, purification, biologic activity, and in vivo application in animals. *J Nucl Med* 1990;31:1501–1509.
9. Krenning EP, Bakker WH, Breeman WAP, et al. Localisation of endocrine-related tumours with radioiodinated analogue of somatostatin. *Lancet* 1989;1:242–244.
10. Watson EE, Stabin M, Bolch WE. Documentation package for MIRDOSE (version 2). Oak Ridge Associated Universities, 1988.
11. International Commission on Radiological Protection. Radiation dose to patients from radiopharmaceuticals. ICRP-publication 53. Oxford: Pergamon Press; 1988.
12. Fleming JS. A technique for the absolute measurement of activity using a gamma camera and computer. *Phys Med Biol* 1979;24:176–180.
13. Myers MJ, Lavender JP, de Oliveira JB, Maseri A. A simplified method of quantitating organ uptake using a gamma camera. *Br J Radiol* 1981;54:1062–1067.
14. Bale WF, Helmkamp RW, Davis TP, et al. High specific activity labeling of protein with ^{131}I by the iodine monochloride method. *Proc Soc Exper Biol & Med* 1966;122:407–414.
15. Lemaire M, Azria M, Dannecker R, Marbach P, Schweitzer A, Maurer G. Disposition of sandostatin, a new synthetic somatostatin analogue, in rats. *Drug Metab Dispos* 1989;17:699–703.
16. Krenning EP, Bakker WH, Kooij PPM, Lameris JS, Reubi JC, Lamberts SWJ. Scintigraphy of various tumours with ^{123}I-labeled Tyr-3-octreotide (T-3-O); a synthetic somatostatin (SMS) analogue [Abstract]. 50th Anniversary of Jules Bordet Institute Symposium on Tumour Targeting, Brus-

sels, 1989.
17. Lamberts SWJ, Krenning EP, Klijn JGM. Clinical applications of somatostatin analogs. *Trends in Endocrinol and Metab* 1990;3:139–144.
18. Lamberts SWJ, Hofland LJ, van Koetsveld PM, et al. Parallel in vivo and in vitro detection of functional somatostatin receptors in human endocrine pancreatic tumors: consequences with regard to diagnosis, localization, and therapy. *J Clin Endocrinol Metab* 1990;71:566–574.
19. Pauw KH, Krenning EP, van Urk H, et al. Scintigraphy of glomus tumors with ^{123}I-labeled Tyr-3-octreotide, a synthetic somatostatin (SMS) analogue [Abstract]. Int Congress Otorhinology, Las Palmas, 1989.

EDITORIAL

Receptors on Tumors Studied with Radionuclide Scintigraphy

In a word, vital phenomena are the result of contact between the organic units of the body and the inner physiologic environment.

Claude Bernard, circa 1865.

In the mid-1800s, a great debate raged among biologists about whether or not a kind of inner force animated and empowered living beings. It was argued that this vital force, the essence of life, existed outside of the natural physical laws governing inanimate objects. Ultimately, scientific evidence revealed something even more miraculous than this, namely that the phenomenon of "living' was based on a complex balance of multiple discrete influences from an inner physiologic environment on the organs, tissues, and cells of the body. In health, these influences result in a "reciprocal harmony" that endows living creatures with a spontaneity of action and a control over the external environment, which is not a property of inorganic objects.

Cancer amounts to a terrible disturbance of the reciprocal harmonies of this internal environment. Certain cells develop a destructive pattern of growth and the ability to metastasize from natural positions within the body to unnatural sites. The basic understanding of the complex derangements that result in a malignant tumor is still incompletely known. However, there is growing evidence for the major role of specific hormones and "growth factors" in promoting and sustaining the malignant state (*1*).

Tumor cell growth may be influenced by hormones and growth factors produced remotely in distant glands and tissues (endocrine effects); by adjacent cells and tissues (paracrine effects); or even by growth factors produced by the tumor cells themselves (autocrine effects) (*2*) (Fig. 1). Certain of these systems such as the effect of estrogen on breast cancer cells, or TGF-alpha, directly stimulate growth by acting at the level of the epidermal growth factor receptor (*3*). Several growth factors are actually inhibitory in action, including somatostatin, TGF-beta, and a 30-kilodalton molecular weight protein that has been recently described to bind to erb-b-2 receptor (*4*).

Such inhibitory substances may potentially have anti-tumor effects. Similarly, antibodies which block growth factor action are also of potential therapeutic importance (*5*).

Sometimes growth factors are previously well-characterized hormones, such as somatostatin, as in the case of the companion article to this editorial (*6*). Somatostatin, a hormone produced in the hypothalamus and the pancreas, has an inhibitory effect on the secretion of many important gastric hormones, including growth hormone, insulin, as well as the secretion of acid by the stomach. Many endocrine-related tumors, including carcinoid tumors, meningiomas, gastrinomas, pancreatic endocrine tumors, and paragangliomas have high affinity receptors for somatostatin (*7*). Direct action of somatostatin on these receptors may have therapeutic benefits by inhibiting tumor growth.

However, somatostatin itself does not have favorable properties as a therapeutic agent, since it is neutralized within a short time after intravenous injection. For this reason, analogues of somatostatin have been developed that have more favorable pharmacokinetics, including a longer duration of action. One of these is the somatostatin analogue octreotide (*8*).

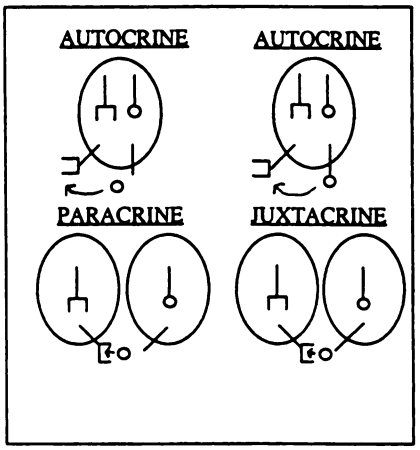

FIGURE 1. Hormonal effects and the "internal environment" in the region of the tumor cell. The cell secretes a growth hormone (O) that interacts with the receptor (U) to stimulate cell growth. Both receptor and hormone are shown with a straight protein tail (—) that represents a protein-connecting piece inserted in the membrane of the tumor cells after manufacture of the hormone or receptor complex by the cell. The hormone may be actively secreted into the external environment of the tumor cell (upper left) and stimulate the receptor directly. Alternatively, the receptor complex may interact with the hormone complex, while both hormone and receptor are fixed in the cell membrane of the tumor cell. These two modes are both "autocrine" effects, since the tumor cell produces a hormone that affects its own growth.